al cortex contain immunoreactive aspartate [4]. In this case, sera may react with both neurotransmitter and metabolic aspartic acid pools, which accounts for the high values [4].

The fact that nerve fibers, synaptic terminals, and axons of giant cells of Betz stain positively for AST indicates that the aspartate is also produced in these structures.

REFERENCES

1. P. A. Motavkin, V. E. Okhotin, and G. Yu. Sulimov, *Arkh. Anat.*, **99**, No. 8, 34-39 (1990).
2. H. Akiyama, T. Kaneko, N. Mizuno, *et al.*, *J. Comp. Neurol.*, **297**, 239-252 (1990).
3. J. P. Donoghue, P. J. Wenthold, and R. A. Altschuler, *J. Neurosc.*, **5**, 2597-2608 (1985).
4. I. Dori, A. Dinopoulos, M. E. Cavanagh, *et al.*, *J. Neurol.*, **319**, 191-204 (1992).
5. T. Kaneko and N. Mizuno, *Ibid.*, **297**, 590-602 (1988).
6. P. Kugler, *Histochemistry*, **87**, 623-625 (1987).
7. R. Martinez-Rodriguez and G. Diaz Arenas, *J. Hirnforsch.*, **29**, 435-441 (1988).
8. Y. Nishimura, M. Natory, and M. Mato, *Brain Res.*, **440**, 144-148 (1988).
9. J. M. Papadimitriou and P. Van Duijn, *J. Cell. Biol.*, **47**, 84-98 (1970).
10. S. B. Tieman, J. H. Neale, and D. G. Tieman, *J. Comp. Neurol.*, **313**, 45-64 (1991).

Ultrastructural, Radioautographic, and Morphometric Analysis of Gastric Mucosa in Chronic Gastritis

V. V. Omigov, D. L. Nepomnyashchikh, and G. A. Lapii

Translated from *Byulleten' Eksperimental'noi Biologii i Meditsiny*, Vol. 122, No. 7, pp. 103-108, July, 1996
Original article submitted July 15, 1995

Biopsy specimens of gastric mucosa from patients with chronic gastritis are examined. The dynamics of structural changes occurring during the development of chronic inflammation is demonstrated and the ultrastructural changes in the mucosa cell populations are described, which together with the radioautographic analysis of biosynthetic reactions and morphometric data characterizes the complex structural and functional rearrangements in the gastric mucosa.

Key Words: *chronic gastritis; gastric biopsy; electron microscopy; radioautography; morphometry*

Gastritis, a process with polymorphic structural manifestations, is the most typical reaction of gastric mucosa in disease. The polymorphism results primarily from the specific combination of destructive and adaptive components [2,3,11,13,14]. The interpretation of structural changes in the gastric mucosa has markedly changed after the investigation into its normal function during eating and between digestion [4,9], which led to the concept of functional morphology of the stomach in health and disease.

Institute of Regional Pathology and Pathomorphology, Siberian Division of the Russian Academy of Medical Sciences, Novosibirsk

In this study biopsy samples of the gastric mucosa obtained during chronic inflammation were studied with the use of complex morphometrical analysis and *in vitro* radioautography.

MATERIALS AND METHODS

The morphology of 230 specimens of the mucosa from the fundal and pyloric regions of the stomach obtained by fibrogastroscopy was analyzed. Light microscopy of paraffin and semithin sections, transmission and scanning electron microscopy, and incubation of biopsy specimens with ^{3}H-uridine and ^{3}H-thymidine to estimate RNA and DNA synthe-

0007-4888/96/0007-0742$15.00

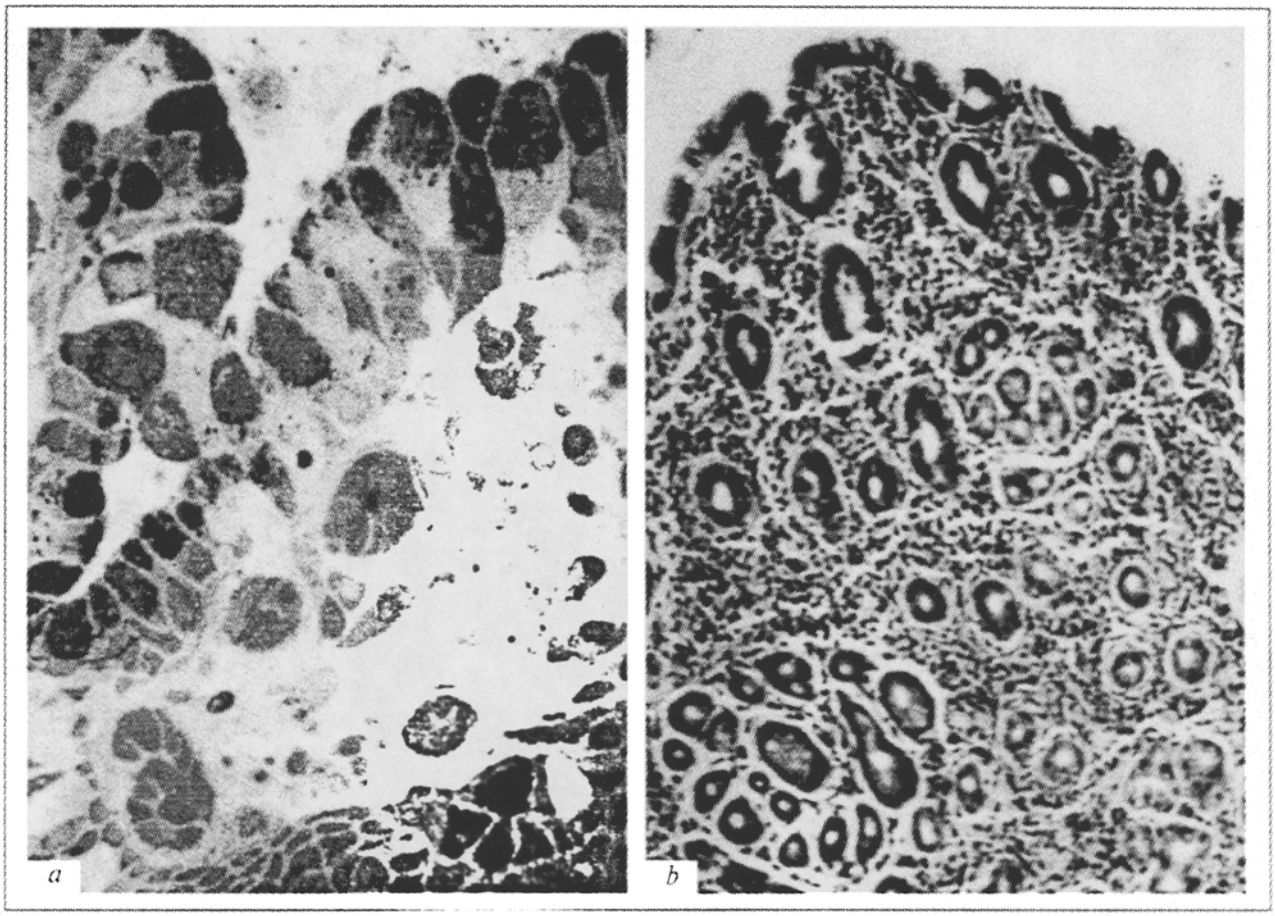

Fig. 1. Microscopic characteristics of gastric biopsy specimens in chronic gastritis. *a*) dystrophy and mosaicism of secretion in the surface epithelium; hyperemia, edema, and slight inflammatory infiltration of the mucosa. Semithin section, PAS reaction, ×800; *b*) diffuse chronic inflammatory cellular infiltration of the mucosa. Hematoxylin and eosin staining. ×200.

sis, respectively, were performed as described elsewhere [5,6].

Stereological analysis of the gastric mucosa was carried out on semithin sections using the multipurpose test system [12]. In order to obtain comparable results the mucosa was arbitrarily divided into surface and deep layers. The primary stereological parameters characterizing structural density of the epithelium, capillaries, and connective tissue were calculated. The secondary parameters, which reflect the parenchymatous-stromal ratio, were calculated from the primary parameters.

The conclusion on the state of the gastric mucosa was based on clinical, endoscopic, and morphological data.

RESULTS

Light microscopy of gastric mucosa showed that the chronic process in the gastric wall starts from catarrhal inflammation followed by the catarrhal-sclerotic and sclerotic (atrophic) stages of gastritis.

The catarrhal stage is characterized by dystrophic changes in the surface epithelium, which are often moderate, but sometimes pronounced. Mucus secretion by mucocytes sometimes varied even in the same biopsy specimen, in which sites with hyper-, hypo-, and normal secretion were seen (Fig. 1, *a*). In the majority of cases, the differentiation into major cell types was preserved in fundal glands; however, dystrophic changes of different degrees were also present.

Dystrophic changes in the surface epithelium, as well as dysplasia and metaplasia, occurred more often and were more pronounced in the pyloric region.

Generally, pyloric glands retained their structure, but dystrophic changes were always present, particularly in older patients. Inflammatory infiltration of the mucosa was similar in cell composition in both regions of the stomach, but its intensity and extension were greater in the pyloric region (Fig. 1, *b*), where sclerotic changes were also more pronounced both in severity and extension. An increase in the severity of sclerotic changes in the gastric

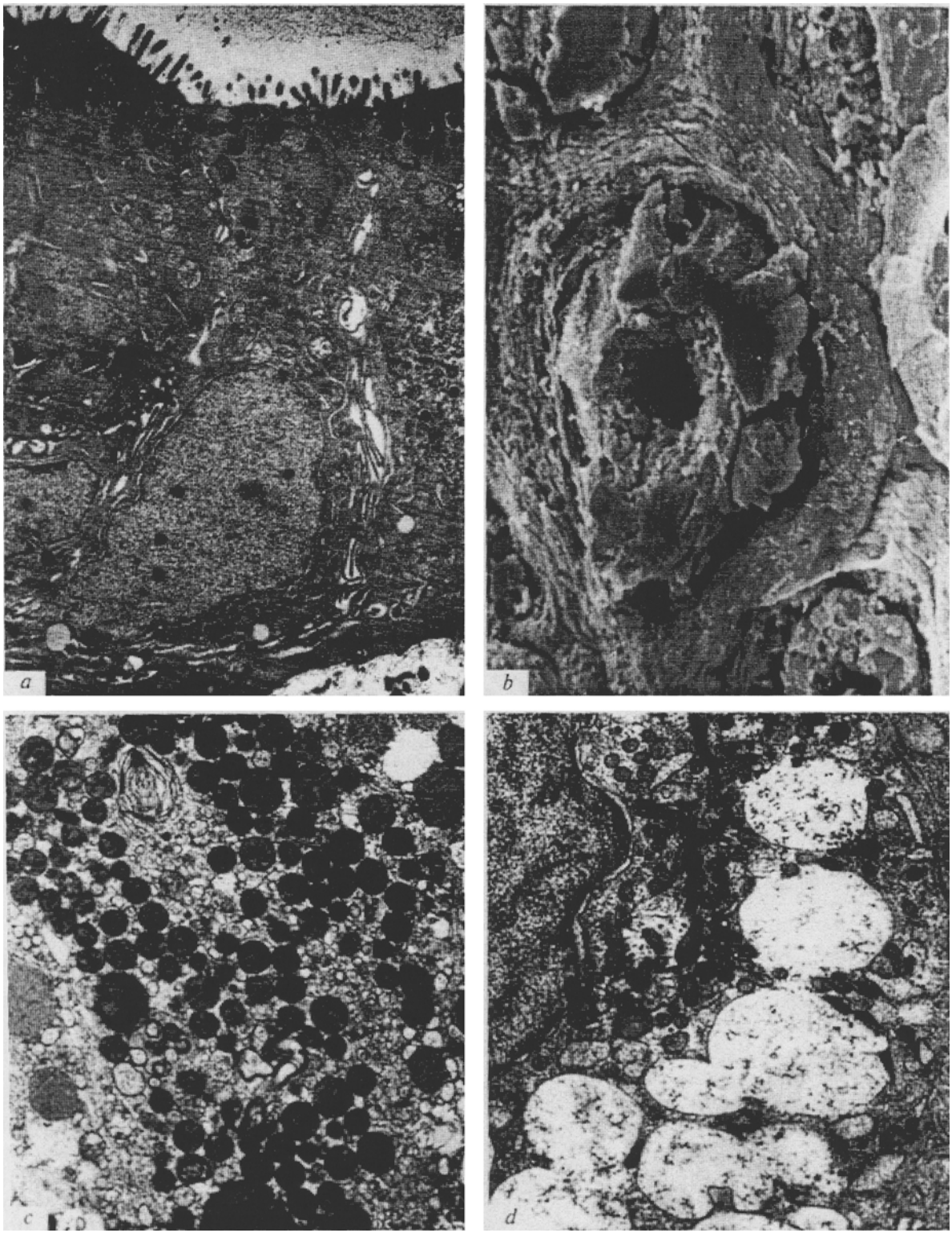

Fig. 2. Ultramicroscopic characteristics of gastric biopsy specimens in chronic gastritis. *a*) surface epithelium cells lacking secretory material. × 3300; *b*) polymorphism of gastric foveae, local accumulations of the mucus. Scanning electron microscopy. × 5000; *c*) fragment of parietal cell: focal extension of the tubulovesicular system, myelin-like structures and autophagosomes in the cytoplasm. × 2600; *d*) fragment of parietal cell: pronounced vascularization of the tubulovesicular system. × 8000.

TABLE 1. Radioautography Analysis of RNA Synthesis in the Gastric Mucosa in Chronic Gastritis

Patients' age	^{3}H-uridine index			
	fundal part		pyloric part	
	SE	endothelium	SE	endothelium
51	-	-	22.8	-
29	-	-	36.0	-
46	-	-	32.1	41.7
42	32.1	19.8	-	-
51	-	-	19.9	51.9
41	23.2	37.7	30.2	39.4
56	44.4	28.0	22.2	14.1
17	60.4	57.2	66.7	66.7
43	86.2	45.4	66.3	28.4
17	-	24.0	72.9	50.8
28	78.4	69.1	72.2	49.5
18	74.5	57.6	63.5	57.4

Note. SE: surface epithelium.

mucosa was paralleled by atrophy of parenchymatous structures and by substantial reduction of their secretory function.

Ultrastructural analysis showed heterogeneous changes in the epithelial structures of the mucosa. The surface epithelium lost the regular monolayer structure, the number of microvilli decreased, and their arrangement disordered. A peculiar feature was the presence of cells of different electron density: electron-transparent with well-structured cytoplasmic organelles and electron-dense with poorly discernible ultrastructural organization. The principal ultrastructural changes of mucocytes included the loss of microvilli, destruction of the cytoskeleton, extrusion of cell contents, and a marked decrease in the intracellular mucin content (Fig. 2, *a*, *b*); the paracellular spaces were unevenly broadened. Ultrastructural changes in the surface epithelium of the pyloric region differed from those in the fundal region by a greater degree of intracellular degeneration, particularly under conditions of lympho- and leukocytic invasion.

TABLE 2. Secondary Stereological Parameters of the Gastric Mucosa in Chronic Gastritis (*M±m*)

Parameter	Fundal region	Pyloric region
Surface layer		
Surface-volume ratio, m^2/cm^3:		
surface epithelium	0.086±0.006	0.107±0.004
capillaries	0.162±0.013	0.181±0.011
capillaries to surface epithelium	0.024±0.002	0.028±0.002
Volume ratio, number of:		
capillaries to surface epithelium	0.121±0.014	0.133±0.013
surface epithelium to stroma	0.528±0.030	0.493±0.032
Deep layer		
Surface-volume ratio, m^2/cm^3, of the:		
glandular epithelium	0.105±0.004	0.128±0.006
capillaries	0.312±0.012	0.486±0.017
capillaries to glandular epithelum	0.015±0.001	0.025±0.002
Volume ratio, number of:		
capillaries to glandular epithelium	0.070±0.006	0.114±0.008
glandular epithelium to stroma	1.318±0.124	0.618±0.058

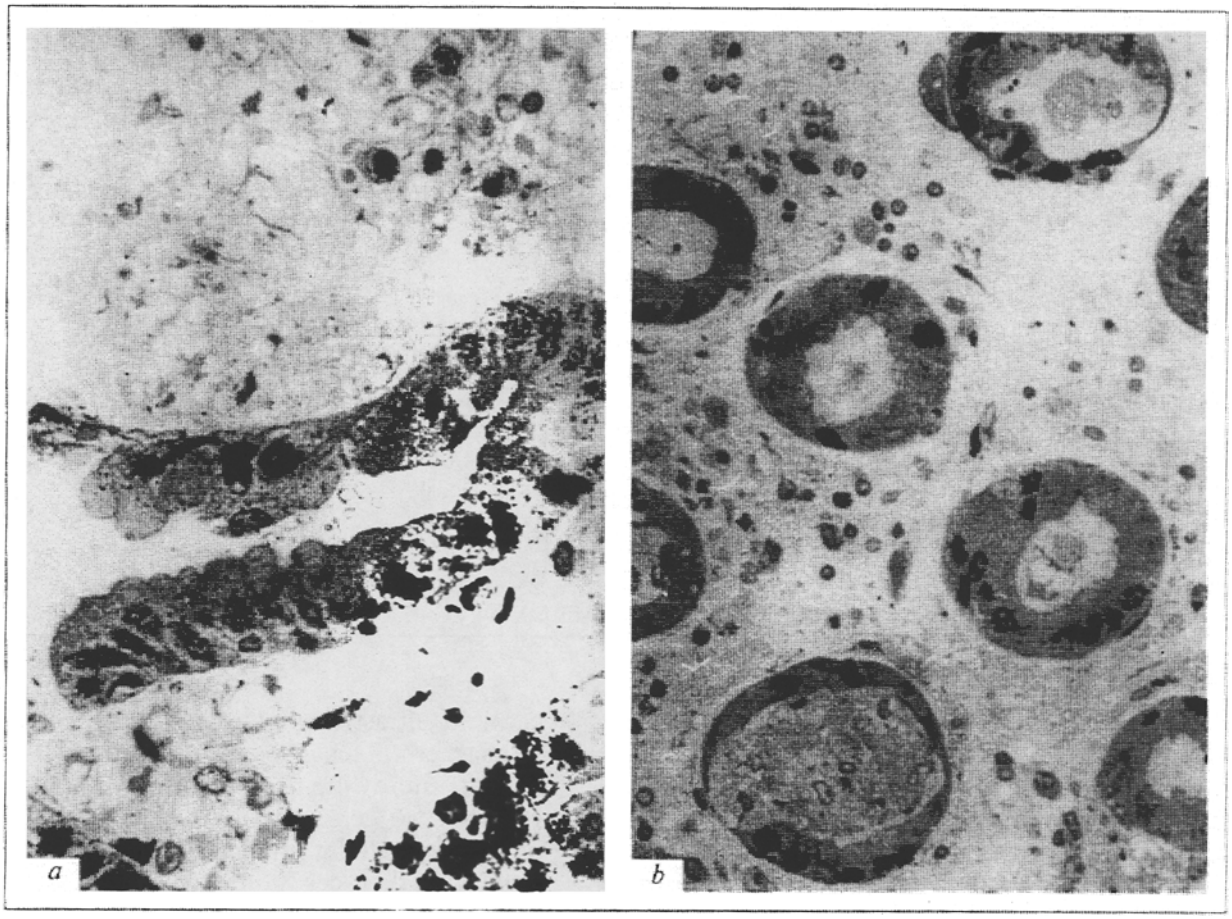

Fig. 3. Radioautographic analysis of gastric mucosa in chronic gastritis. *a*) RNA synthesis in the surface epithelium. Semithin section. Incubation with ^{3}H-uridine. Azure II staining. × 800. *b*) DNA synthesis in foveolar epitheliocytes. Semithin section. Incubation with ^{3}H-thymidine. × 500.

The parietal cells showed the highest degree of ultrastructural polymorphism. Epitheliocytes of two morphological types and probably with different functional activity were revealed. Some cells had light nuclei rich in euchromatin, well-developed intracellular canaliculi, and numerous mitochondria with slightly clarified matrix. Others were parietal glandulocytes with electron-dense nuclei and cytoplasm containing densely packed mitochondria, large autophagosomes with myelin-like structures, and well-developed system of intracellular canaliculi. The most typical change in the structure of parietal cells was extension and deformation of the tubulovesicular system (Fig. 2, *c*, *d*).

In contrast to parietal cells, the population of the chief cells of the fundal glands was virtually not polymorphous. Glandulocytes of this type had oval-rounded nuclei with great amounts of heterochromatin, numerous light secretory granules in the cytoplasm, elements of the rough endoplasmic reticulum, and few mitochondria with a rather dense matrix. In some cells, deposits of glycogen granules, occasional lysosomes, autophagosomes, and myelin-like structures were seen. The damage to chief cells was associated with their detachment from the basal membrane and the appearance of polymorphic autophagosomes in the cytoplasm. In some zymogenous elements the cytoplasm was almost completely filled with secretory granules fused in a single conglomeration, which caused the displacement of the nuclei towards the basal pole. The nuclei appeared deformed and pyknotic; some chief epitheliocytes were partially or totally necrotic.

Radioautographic analysis of the RNA synthesis in the surface epithelium (Table 1) revealed substantial variations of metabolic activity in both regions of the stomach (Fig. 3, *a*). The ^{3}H-uridine index in epitheliocytes varied from 19.9 to 86.2%.

Generally, the biosynthetic activity of epithelial cells of the fundal and pyloric regions was synchronous: the highest and the lowest indexes of ^{3}H-uridine-labeled cells were recorded simultaneously. In addition, the metabolic activity of epitheliocytes correlated with that of blood capillary endothelio-

cytes, in which the ^{3}H-uridine index varied from 14.1 to 69.1%. Comparative analysis showed that the level of biosynthetic activity in epitheliocytes depends on the duration of the process and the patient's age.

Proliferative activity was observed mainly in the foveal epitheliocytes (Fig. 3, *b*), and sometimes high ^{3}H-thymidine index was recorded in dystrophic atrophic germinal epithelium, this reflecting the focal induction of cell regeneration processes. Individual differences in the proliferative activity of epitheliocytes in the fundal and pyloric regions were observed (from 2.2 to 29.8%), the low values reflecting the development of atrophy.

Tissue stereological analysis of biopsy specimens in chronic inflammation has demonstrated a principal similarity in spatial organization of the mucosa in both regions of the stomach (Table 2). Quantitative parameters characterize a better vascularization of the mucosa in the pyloric region in general. This is reflected in the level of structural density of the capillaries, their surface/volume ratio, and the capillary-epithelium interactions.

Thus, complex morphological study of gastric mucosa in chronic inflammation showed polymorphism of changes, which reflects a combination of tissue, cell, and intracellular reactions [1,8] and typical compensatory adaptive processes [7]. Degenerative dystrophic changes in the surface and glandular epithelial cells with secretory disorders and development of stromal sclerosis are the main compensatory-adaptive reactions. It is noteworthy that the high level of biosynthetic reactions is retained in the damaged surface epithelium [10], and the specific spatial organization of the microcirculatory bed provides for a long functioning of the stomach under conditions of chronic inflammation [8].

REFERENCES

1. L. I. Aruin, in: *Structural Basis of Adaptation and Compensation of Impaired Functions. A Manual* [in Russian], D. S. Sarkisov (ed.), Moscow (1987), pp. 185-263.
2. L. I. Aruin, P. Ya. Grigor'ev, V. A. Isakov, and E. P. Yakovenko, *Chronic Gastritis* [in Russian], Amsterdam (1993).
3. V. B. Zolotarevskii and A. G. Ufimtseva, *Arkh. Pat.*, No. 6, 62-66 (1994).
4. Yu. M. Lazovskii, *Functional Morphology of the Stomach in Health and Pathology* [in Russian], Moscow (1947).
5. G. A. Lapii and G. I. Nepomnyashchikh, *Byull. Eksp. Biol. Med.*, **118**, No. 8, 198-202 (1994).
6. D. L. Nepomnyashchikh, *Ibid.*, 190-193.
7. D. S. Sarkisov, *Essays on the History of General Pathology* [in Russian], Moscow (1993).
8. A. M. Ugolev, *Evolution of Digestion and Principles of Evolution of Functions* [in Russian], Leningrad (1985).
9. V. M. Uspenskii, *Functional Morphology of the Gastric Mucosa* [in Russian], Leningrad (1986).
10. E. E. Deschner, S. J. Winawer, and M. Lipkin, *J. Natl. Cancer Inst.*, **48**, 1567-1574 (1972).
11. J. O. Gebbers and J. A. Laissue, *Microecol. Ther.*, **14**, 137-168 (1984).
12. E. R. Weibel, G. S. Kistler, and W. R. Scherle, *J. Cell. Biol.*, **30**, 23-28 (1966).
13. B. Wolf, E. Muller, and A. Schwindle, *Virchow's Arch. [A]*, **407**, 209-219 (1985).
14. J. I. Wyatt and M. F. Dixon, *J. Pathol.*, **154**, 113-124 (1988).